



## OPEN

Diosgenin-induced cognitive enhancement in normal mice is mediated by 1,25D<sub>3</sub>-MARRSChihiro Tohda<sup>1</sup>, Young-A Lee<sup>2</sup>, Yukiori Goto<sup>2</sup> & Ilka Nemere<sup>3</sup>SUBJECT AREAS:  
NATURAL PRODUCTS  
LONG-TERM MEMORY  
DRUG DEVELOPMENTReceived  
1 October 2013Accepted  
14 November 2013Published  
2 December 2013Correspondence and  
requests for materials  
should be addressed to  
C.T. (chihiro@inm.u-  
toyama.ac.jp)

<sup>1</sup>Division of Neuromedical Science, Department of Bioscience, Institute of Natural Medicine, University of Toyama, 2630 Sugitani, Toyama 930-0194, Japan, <sup>2</sup>Primate Research Institute, Kyoto University, Inuyama, Aichi 484-8506, Japan, <sup>3</sup>Department of Nutrition, Dietetics, and Food Sciences, Utah State University, Logan, Utah 84322, USA.

We previously reported that diosgenin, a plant-derived steroidal sapogenin, improved memory and reduced axonal degeneration in an Alzheimer's disease mouse model. Diosgenin directly activated the membrane-associated rapid response steroid-binding receptor (1,25D<sub>3</sub>-MARRS) in neurons. However, 1,25D<sub>3</sub>-MARRS-mediated diosgenin signaling was only shown *in vitro* in the previous study. Here, we aimed to obtain *in vivo* evidence showing that diosgenin signaling is mediated by 1,25D<sub>3</sub>-MARRS in the mouse brain. Diosgenin treatment in normal mice enhanced object recognition memory and spike firing and cross-correlation in the medial prefrontal cortex and hippocampal CA1. In diosgenin-treated mice, axonal density and *c-Fos* expression was increased in the medial prefrontal and perirhinal cortices, suggesting that neuronal network activation may be enhanced. The diosgenin-induced memory enhancement and axonal growth were completely inhibited by co-treatment with a neutralizing antibody for 1,25D<sub>3</sub>-MARRS. Our *in vivo* data indicate that diosgenin is a memory-enhancing drug and that enhancement by diosgenin is mediated by 1,25D<sub>3</sub>-MARRS-triggered axonal growth.

Many scientific reports have shown a variety of pharmacological effects for natural compounds. However, few studies have successfully identified a direct target of the compound. We previously reported that diosgenin, a plant-derived steroidal sapogenin, improved memory function and reduced axonal degeneration in an Alzheimer's disease (AD) mouse model, 5XFAD. We showed that diosgenin directly activated the membrane-associated rapid response steroid-binding receptor (1,25D<sub>3</sub>-MARRS) in neurons<sup>1</sup>. Several biological effects of diosgenin have been reported, including anti-cancer effects<sup>2</sup>, anti-food allergy effects<sup>3</sup>, improvement of aging-related cognitive deficits<sup>4</sup> and relief of diabetic neuropathy<sup>5</sup>. Although several signaling pathways have been reported to be activated by diosgenin, including STAT3 inhibition<sup>6</sup> and activation of Akt<sup>7</sup>, a direct binding target had not been reported.

1,25D<sub>3</sub>-MARRS was identified as a cell surface receptor for 1 $\alpha$ ,25-dihydroxyvitamin D<sub>3</sub> (DHVD3) that mediates rapid non-genomic responses. The receptor facilitates various signaling pathways, including the activation of PKC<sup>8-10</sup>, PKA<sup>8,11</sup>, ERK<sup>9</sup> and PI3K<sup>12</sup> and sequestering of STAT3<sup>13</sup> in intestinal and osteoblast cells. However, the functional roles of 1,25D<sub>3</sub>-MARRS in the nervous system had not been demonstrated before our study. Despite the importance of DHVD3 as a hormone, studies of the DHVD3 signaling pathway have mainly focused on nuclear vitamin D receptor (nVDR) rather than 1,25D<sub>3</sub>-MARRS because DHVD3 may primarily stimulate the nuclear receptor nVDR, which operates through binding to DNA and activating gene expression<sup>14</sup>. Physiologically, the dominant conformation state of DHVD3 is 6-*s-trans*, which causes it to associate with nVDR<sup>15</sup>. In contrast, diosgenin is not involved in nVDR signaling<sup>1</sup>. Therefore, diosgenin signaling likely does not overlap with DHVD3 signaling.

We found that the 1,25D<sub>3</sub>-MARRS pathway was activated by diosgenin and led to axonal growth in neurons<sup>1</sup>. However, this signaling pathway was shown using only primary cultured cortical neurons, not *in vivo* studies. Therefore, in this study, we aimed to obtain *in vivo* evidence showing that diosgenin signaling is mediated by 1,25D<sub>3</sub>-MARRS in the mouse brain.

In 5XFAD mice, diosgenin reduced amyloid plaques and hyperphosphorylated tau in the brain<sup>1</sup>. However, we hypothesized that the most significant effect of diosgenin was eliciting axonal growth. If this result was found, normal cognitive function could also be enhanced by the axonal growth-promoting effects of diosgenin. Thus,



this study may provide an important perspective on the relationships between axonal growth and cognitive function.

## Results

To investigate the effect of diosgenin on cognitive function in normal young mice, diosgenin or vehicle solution was administered i.p. to mice for 7 days. Used dose of diosgenin ( $10 \mu\text{mol}/\text{kg} = 4.14 \text{ mg}/\text{kg}$ ) was similar to one used in 5XFAD mice. At drug administration day 5, a training session in object recognition test was performed, and after a 48 h interval, a test session in the test was performed. We previously confirmed that normal mice could not keep object recognition memory with an interval time longer than 24 h. As shown in Figure 1A, diosgenin treatment significantly enhanced object recognition memory in normal mice. On session days, diosgenin was administered 1 h before a training session (day 5) and 1 h before a test session (day 7). This administration protocol suggested that diosgenin may temporarily stimulate neurons related to memory acquisition and/or memory retention. Therefore, as shown in Figure 1B, the final diosgenin injection was administered at day 5, 1 h before a training session. Even when diosgenin was not administered on the testing day, treatment significantly enhanced object recognition memory in normal mice. These data suggest that when administered before the training session, diosgenin treatment enhanced neuronal circuit function or morphology, which reinforced object recognition memory.

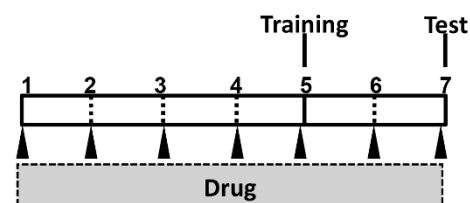
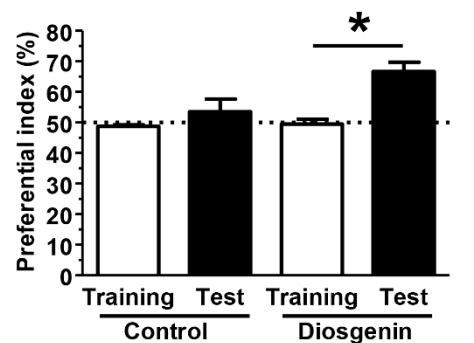
We examined modulation of spike firing activity in the medial prefrontal cortex (mPFC) and hippocampal CA1 of mice under urethane anesthesia. Spike firing of mPFC and CA1 neurons were recorded in vehicle-treated and diosgenin-treated mice. Significant increases of spike firing frequency (Figure 2A) and percentage of spike occurring as bursts (Figure 2B) were observed in the mPFC of diosgenin-treated mice. In the CA1, spike firing frequency was significantly enhanced in diosgenin-treated mice. Synchronous activity of spike firing between mPFC and CA1 was evaluated using cross-correlation analysis (Figure 2C). Diosgenin treatment significantly increased synchronized spike firing discharges between mPFC and CA1 neurons.

As shown in our previous study, diosgenin treatment increased axonal growth in primary cultured mouse cortical neurons<sup>1</sup>. Diosgenin-induced axonal growth was completely inhibited by knockdown of  $1,25\text{D}_3\text{-MARRS}$  by siRNA transfection<sup>1</sup>. In this study, we confirmed that diosgenin-induced axonal growth in normal neurons was also inhibited by a neutralizing antibody specific to  $1,25\text{D}_3\text{-MARRS}$ . Four days after diosgenin treatment ( $1 \mu\text{M}$ ), axonal density in cortical neurons was significantly increased (Figure 3). Pretreatment with anti- $1,25\text{D}_3\text{-MARRS}$  ( $1:500$  dilution) for 15 min completely inhibited diosgenin-induced axonal growth. This result indicates that masking  $1,25\text{D}_3\text{-MARRS}$  blocks the diosgenin pathway that leads to axonal growth in normal neurons.

Next, we investigated *in vivo* if  $1,25\text{D}_3\text{-MARRS}$  mediated diosgenin signaling in the brain. Artificial CSF (aCSF) or an anti- $1,25\text{D}_3\text{-MARRS}$  antibody in aCSF was continuously infused into the lateral ventricle of normal mice. Diosgenin or vehicle solution was administered i.p. to the mice. Immediately before the training session, locomotion was measured. There were no significant differences between groups in distance moved for 10 min (Figure 4B). On day 5, an object recognition memory test was conducted. Control mice that received aCSF and vehicle solution showed no increase in the preferential index. However, mice infused with aCSF and injected with diosgenin for 6 days performed significantly above-chance exploratory behavior in the presence of a novel object (Figure 4A). In contrast, chronic intracerebroventricular infusion of a neutralizing antibody for  $1,25\text{D}_3\text{-MARRS}$  completely inhibited diosgenin-induced memory enhancement (Figure 4A).

At 60 min after the novel object recognition test, the brains of the mice were removed for immunohistochemistry because c-Fos

A)



B)

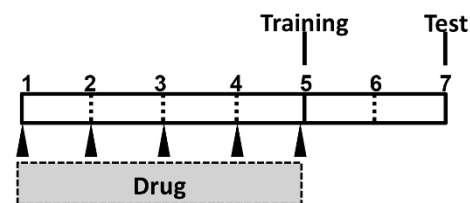
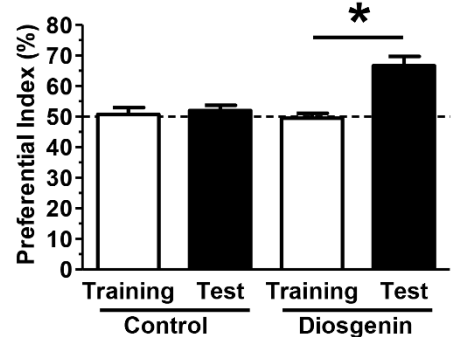


**Figure 1 | Effects of diosgenin on object recognition memory in normal mice.** (A) Diosgenin ( $10 \mu\text{mol}/\text{kg}$ , i.p.) or vehicle solution was administered for 7 days to mice (males, 6 weeks old). On administration day 5, an object recognition test was started. The preference indices of the training and test sessions are shown. (\* $p < 0.05$ , two-tailed paired  $t$ -test;  $n = 3-5$  mice). (B) Diosgenin ( $10 \mu\text{mol}/\text{kg}$ , i.p.) or vehicle solution was administered for 5 days to mice (males, 6 weeks old). One hour after the last administration on administration day 5, an object recognition test was initiated. The preference indices of the training and test sessions are shown. (\* $p < 0.05$ , two-tailed paired  $t$ -test;  $n = 3-5$  mice).

expression in the perirhinal cortex was transiently activated and peaks 60 min after the test session in our preliminary data. Brain slices were prepared for quantification of axonal density and neuronal activation. We measured the lengths of phosphorylated neurofilament H (pNF-H)-positive axons in the mPFC, perirhinal cortex and hippocampal areas CA1 and CA3. In the mPFC (Figure 5A) and

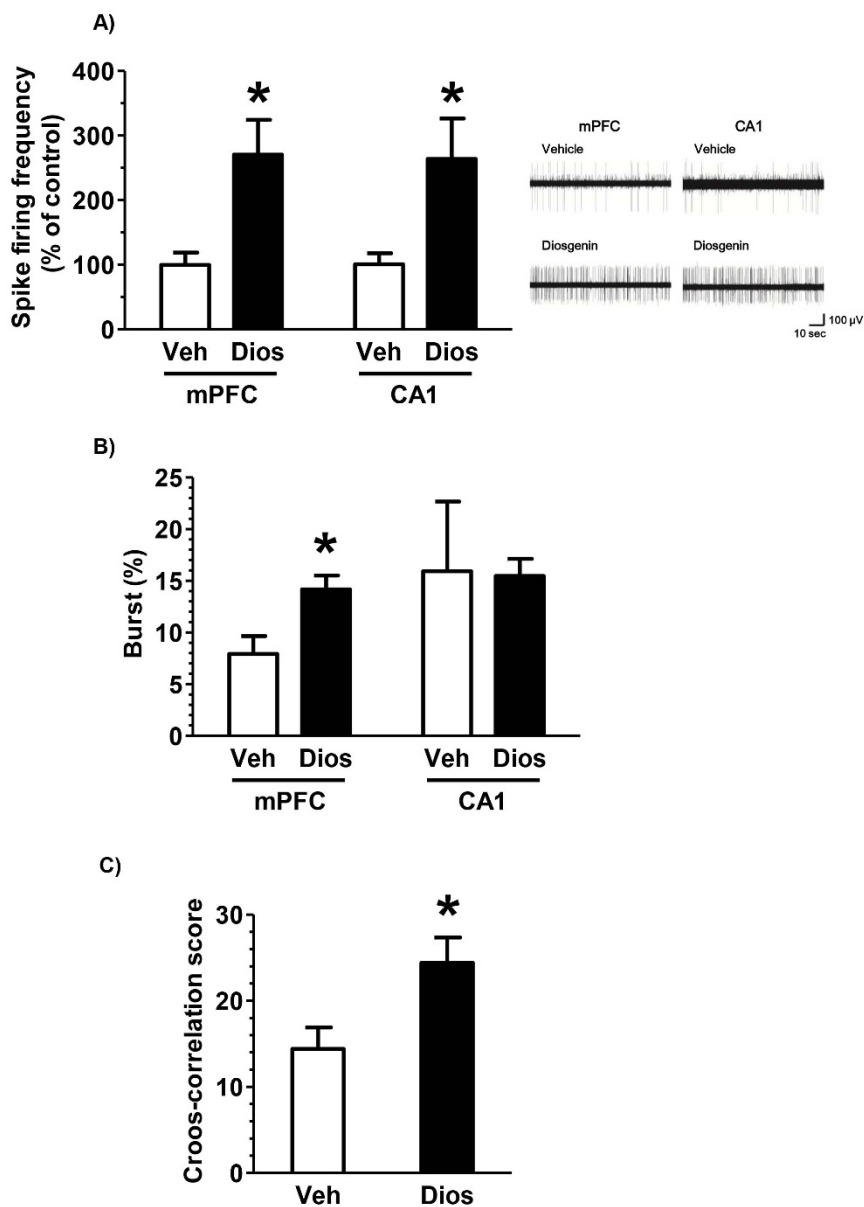


**Figure 2 | Effect of diosgenin on spike firing of the mPFC and CA1 neurons.** Diosgenin (10  $\mu$ mol/kg, i.p.) or vehicle solution was administered for 21 days to mice (males, 8 weeks old). The next day of the last administration day, an *in vivo* electrophysiological recording was performed under urethane anesthesia. (A) Spike firing frequencies and representative spike charts, (B) the percentage of bursts in firings were recorded from the mPFC and CA1. (C) Cross-correlation scores between the mPFC and CA1 were recorded in vehicle- or diosgenin-treated mice. (\* $p < 0.05$ , two-tailed paired *t*-test;  $n = 6$  mice).

perirhinal cortex (Figure 5B), axonal densities were significantly increased in aCSF-infused and diosgenin-treated mice. The increased axon density was almost completely reduced in anti-1,25D<sub>3</sub>-MARRS antibody infused mice (Figures 5A, 5B and 5E). In contrast, axonal density in hippocampal areas CA1 (Figure 5C) and CA3 (Figure 5D) was not increased by diosgenin administration in aCSF-infused mice. Infusion of an anti-1,25D<sub>3</sub>-MARRS antibody also produced no changes in hippocampal axon growth.

c-Fos expression provides information about which brain areas are activated after a certain event. We previously confirmed that c-Fos expression in the brain peaked at 60 min after the test session of the object recognition test. Following aCSF infusion, c-Fos expression in the mPFC (Figure 6A), CA1 (Figure 6C), CA3 (Figure 6D) and especially in the perirhinal cortex (Figure 6B) was increased in diosgenin-treated mice. The diosgenin-stimulated increase in c-Fos-positive neurons in the perirhinal cortex was significantly decreased by

anti-1,25D<sub>3</sub>-MARRS antibody infusion (Figures 5B and 5C). In the mPFC and CA1, a trend towards a reduction in c-Fos was shown following antibody infusion (Figures 6A, 6C and 6E), but not in CA3.

## Discussion

Diosgenin administration to normal mice enhanced object recognition memory and axonal density in the mPFC and perirhinal cortex (Figure 5A and 5B). In those regions, c-Fos expression was increased in diosgenin-treated mice (Figure 6A and 6B), suggesting that neuronal network activation may be enhanced in the mice. Although axonal growth was not observed in hippocampal CA1 (Figure 5C) and CA3 (Figure 5D), c-Fos expression tended to be increased in CA1 of diosgenin-treated mice (Figure 6C). In addition, frequencies of spike firing in the mPFC and CA1 (Figure 2A) and synchronization of spikes between mPFC and CA1 (Figure 2C) were clearly shown in diosgenin-treated mice by *in vivo* electrophysio-

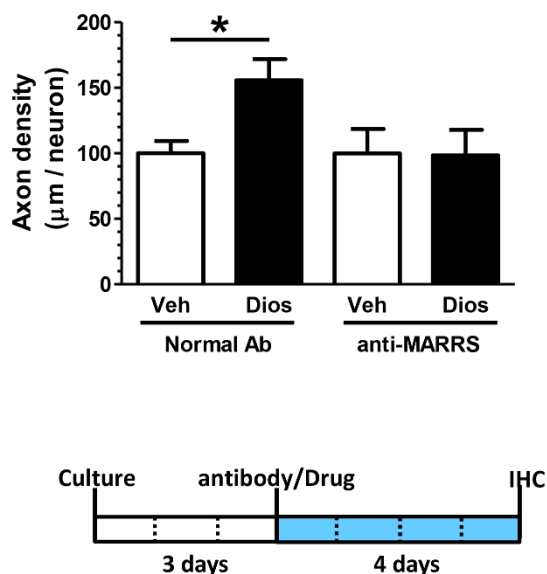


**Figure 3** | Effect of a neutralizing antibody to 1,25D<sub>3</sub>-MARRS on diosgenin-induced axonal outgrowth. Mouse cortical neurons were pretreated with normal IgG or an anti-1,25D<sub>3</sub>-MARRS antibody. Fifteen minutes later, diosgenin (1 µM) or vehicle solution was added to the cells. Four days after drug administration, the cells were fixed and double-immunostained for pNF-H and MAP2. The density of pNF-H-positive axons per MAP2-positive neuron was quantified for each treatment (\**p* < 0.05, two-tailed unpaired *t*-test, *n* = 21).

logical approaches. *In vivo* physiological study by Benedetti et al. suggests that the expression of *c-Fos* is related to excitatory synaptic input<sup>16</sup>. The diosgenin-induced memory enhancement and axonal growth were completely inhibited by co-treatment with a neutralizing antibody against 1,25D<sub>3</sub>-MARRS. Our *in vivo* data indicate that memory enhancement by diosgenin may be mediated by 1,25D<sub>3</sub>-MARRS-triggered axonal growth.

In this study, diosgenin administration may have strengthened the neuronal network before starting the object recognition memory test. Even when administration was halted before the training session (Figure 1B), memory enhancement by diosgenin was similar to when administration was continued until 1 day after (Figure 4A) and 2 days after (Figure 1A) the training session. These data suggest that in response to 5 days of diosgenin treatment, the neuronal network for memory formation may be reinforced. Our unpublished results showed that only 1-day treatment with diosgenin was not enough to enhance the object recognition memory. It means that diosgenin may require a certain duration for providing neurons for some changes, or repeated treatment may be necessary to gain memory enhancement.

There are a few reports of memory activators in normal animals, such as estradiol injection<sup>17</sup>, HGF transgenes<sup>18</sup>, i.c.v. injection of recombinant Reelin protein<sup>19</sup> and p.o. administration of the curcumin derivative J147<sup>20</sup>. Those studies demonstrated that treatments increased spine density but did not show axonal changes. The present data suggest that axonal growth can be facilitated even in adult animals, and an increase in axonal density may positively regulate cognitive function.

1,25D<sub>3</sub>-MARRS has many synonyms, including Pdia3, ERp57 and GRP58. Pdia3 protein expression in the human brain is strong in cerebral cortical neurons but moderate in hippocampal neurons<sup>21</sup>, which may be one reason why diosgenin activates axonal growth predominantly in the cerebral cortex. Elevated axonal density could lead to an increase in neuronal connections, resulting in higher *c-Fos* expression and spike firing. As shown in our previous study, diosgenin-induced axonal growth is mediated by PI3K, ERK, PKC and

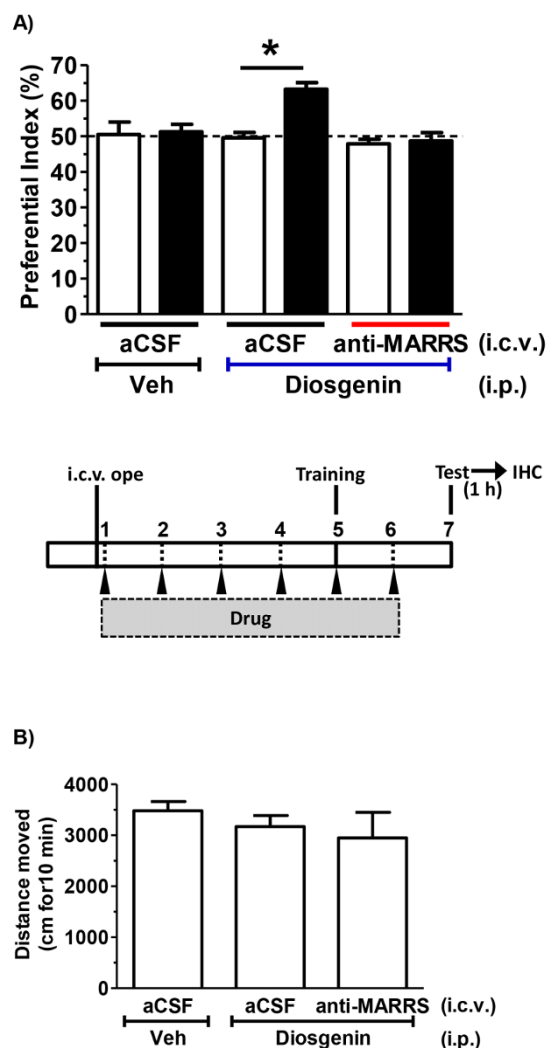


**Figure 4** | Effect of a neutralizing antibody to 1,25D<sub>3</sub>-MARRS on diosgenin-induced memory enhancement. aCSF or an anti-1,25D<sub>3</sub>-MARRS antibody in aCSF was chronically infused into the lateral ventricle of normal mice (males, 6 weeks old) using a mini-osmotic pump. Diosgenin or vehicle solution was i.p. injected for 6 days. On administration day 5, the training session of the object recognition memory test was conducted. After 48 h, a test session was carried out. (A) The preferential indices of the training (open columns) and test (closed columns) sessions are shown. (\**p* < 0.05, two-tailed paired *t*-test; *n* = 4–6 mice). (B) At administration day 5, locomotion in an open field was measured. Distances moved over 10 min are shown.

PKA<sup>1</sup>, among others. The PI3K-Akt pathway is known to regulate local protein translation via the mTOR pathway, thus playing an important role in axon regeneration<sup>22</sup>. PI3K also regulates Cdc42, which is a key regulator of cytoskeletal reorganization in axonal tips<sup>23</sup>. ERK signaling is also required for local axon assembly<sup>24</sup> and local protein translation at the growth cone<sup>25</sup>. The phosphorylation of GAP-43 by PKC in growth cones is required for axonal outgrowth<sup>26</sup>. The PKA pathway is also known to be associated with axonal extension in cortical neurons<sup>27</sup>.

DHVD3 is a physiological and endogenous ligand of 1,25D<sub>3</sub>-MARRS. Although DHVD3 was reported to affect neurite outgrowth in embryonic rat hippocampal neurons, it is unknown whether the effect is mediated by 1,25D<sub>3</sub>-MARRS or nVDR<sup>28</sup>. In addition, there are several reports showing negative effects of DHVD3 on cognitive function. When adult rats (6 months old) were administered DHVD3 for 21 days, cognitive function was not altered<sup>29</sup>. In human

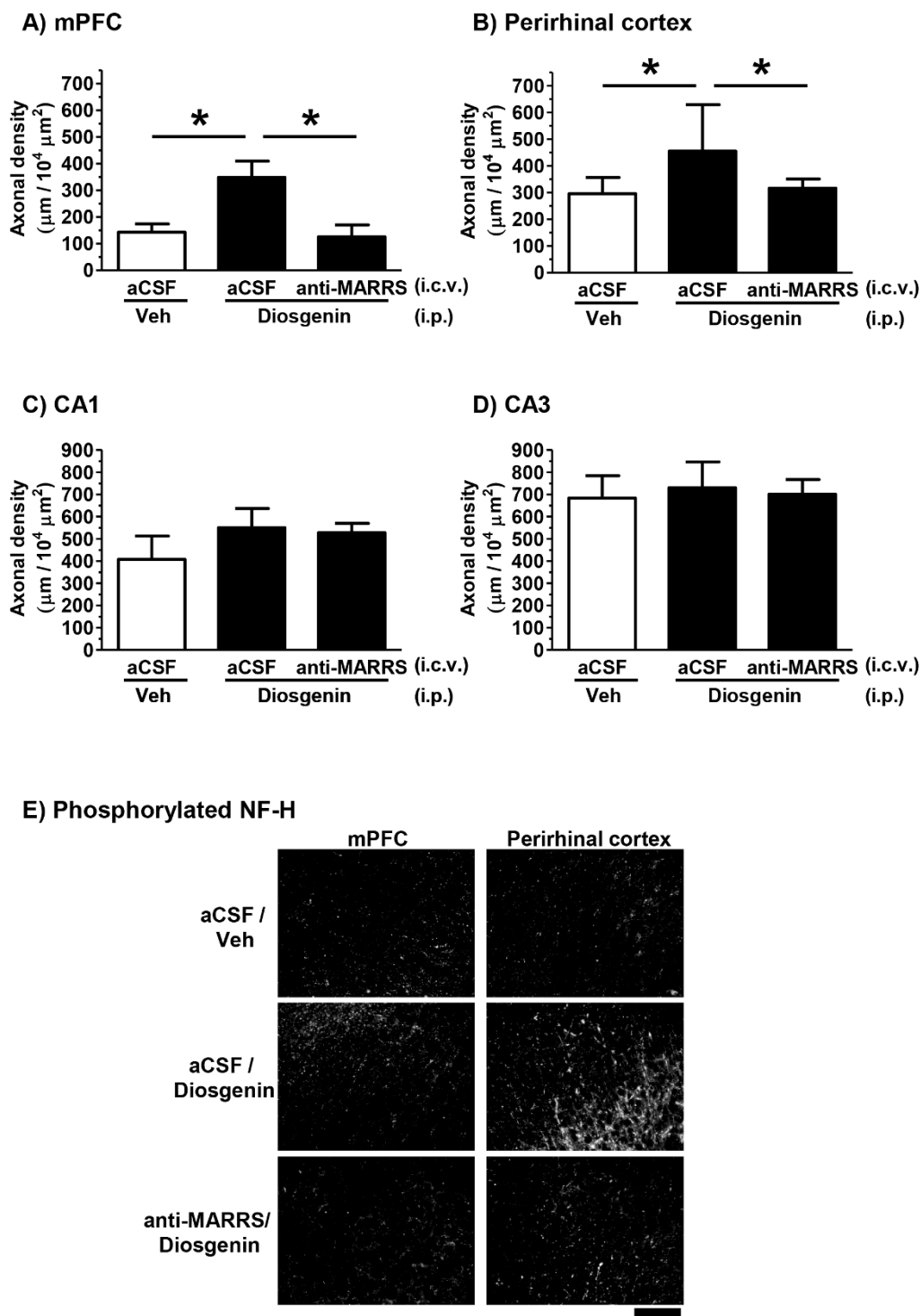


**Figure 5** | Effects of diosgenin and neutralization of 1,25D<sub>3</sub>-MARRS on axonal density in the normal mouse brain. Immunohistochemistry for pNF-H was carried out. Total lengths of pNF-H positive axons in the mPFC (A), perirhinal cortex (B) and hippocampal CA1 (C) and CA3 (D) were quantified and are shown as µm per 10,000 µm<sup>2</sup> area. Representative images of the mPFC and perirhinal cortex are shown in (E). Scale bar = 100 µm. (\**p* < 0.05, one-way ANOVA *post hoc* Dunnett's test, *n* = 4–6).

young adults, DHVD3 supplementation also did not alter cognitive function<sup>30</sup>. The conformation of DHVD3 is flexible, and approximately 95% of DHVD3 exists in the non-steroidal and extended 6-*s*-trans form<sup>15,31</sup>. In addition, DHVD3 is metabolized to 1 $\alpha$ ,24,25-dihydroxyvitamin D<sub>3</sub>, and its biological concentration is strictly controlled<sup>32</sup>. Taken together, our data suggest that activation of 1,25D<sub>3</sub>-MARRS elicits cognitive enhancement and that exogenous administration of diosgenin effectively improves memory.

## Methods

All experiments were performed in accordance with the Guidelines for the Care and Use of Laboratory Animals of the Sugitani Campus of the University of Toyama. All protocols were approved by the Committee for Animal Care and Use of the Sugitani Campus of the University of Toyama. The approval number for the animal experiments is A2011-INM1. All efforts were made to minimize the number of animals used.

**Materials.** Diosgenin (Wako, Osaka, Japan) was dissolved in ethanol at 10-fold the final concentration, and the stock solution was diluted in a 5% glucose aqueous

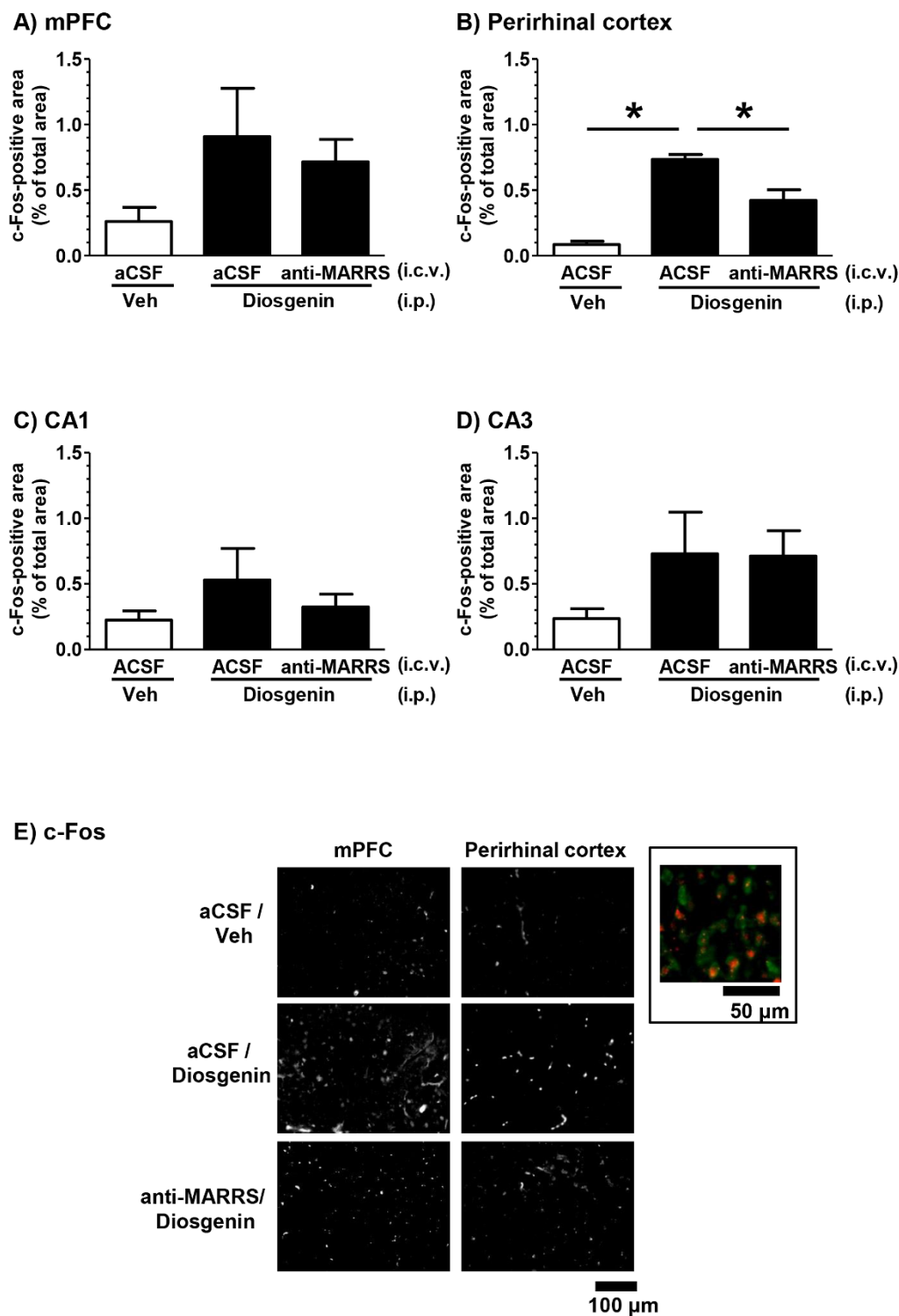


**Figure 6** | Effects of diosgenin and neutralization of 1,25D<sub>3</sub>-MARRS on c-Fos expression in the normal mouse brain. Immunohistochemistry for c-Fos was carried out. c-Fos-positive areas in the mPFC (A), perirhinal cortex (B), CA1 (C) and CA3 (D) were quantified and shown as a percent of total area. Representative images of the mPFC and perirhinal cortex are shown in (E). Scale bar = 100  $\mu$ m. Inside a box, c-Fos expression (red) and neuronal cell bodies traced by NeuroTrace Fluorescent Nissl Stains (green) were merged. Scale bar = 50  $\mu$ m. c-Fos is localized in neurons. (\* $p < 0.05$ , one-way ANOVA *post hoc* Dunnett's test,  $n = 4-6$ ).

solution. The vehicle solution was 10% ethanol in 5% glucose. A specific neutralizing antibody for 1,25D<sub>3</sub>-MARRS (clone Ab099) was provided as a gift by Dr. Nemere.

**Animals.** Male ddY mice (6 weeks old, Japan SLC, Shizuoka, Japan) were housed with free access to food and water and kept in a controlled environment ( $22 \pm 2^\circ\text{C}$ ,  $50 \pm 5\%$  humidity, 12-h light cycle starting at 7:00 am). The drug or vehicle solution was intraperitoneally administered once a day for 5 days (Figure 1B), 6 days (Figure 3) or 7 days (Figure 1A).

**Open field test.** On the day before a training session, mice were individually habituated to an open-field box (30 cm  $\times$  40 cm; height, 36.5 cm) for 10 min, and their paths were tracked by a digital camera. The distance moved for 10 min was analyzed using the locomotion activity function of EthoVision 3.0 (Noldus, Wageningen, Netherlands). Testing was carried out in a dimly illuminated room (90 lux).

**Object recognition test.** Two identical objects (colored ceramic ornaments) were placed at a fixed distance within a square box (30 cm  $\times$  40 cm; height, 36.5 cm,



90 lux). A mouse was then placed at the center of the box, and the number of times it made contact with the two objects was recorded during a 10-min period (training session). Mice were then placed back into the same box 48 h after the training session, and one of the objects used during the training session was replaced with a novel object (another ceramic ornament with a different shape and color). The mice were then allowed to explore freely for 10 min; the number of times they made contact with each object was recorded (test session). A preference index, defined as the ratio of the number of times a mouse made contact with any of the objects (training session) or the novel object (test session) over the total number of times the mouse made contact with both objects, was used to measure cognitive function for objects.

**Immunohistochemistry.** Precisely 60 min after the novel object recognition test session, mice were anesthetized and transcardially perfused with cold physiological saline. The brains were carefully removed from the skull, immediately immersed in 30% sucrose-PBS and stored at  $-30^{\circ}\text{C}$ . The brains were cut into 20  $\mu\text{m}$  coronal slices every 100  $\mu\text{m}$  in the medial prefrontal cortex area (bregma + 1.70 to + 2.46 mm) and the perirhinal cortex area (bregma  $-1.34$  to  $-2.06$  mm) using a cryostat (CM3050S, Leica, Heidelberg, Germany). The slices were fixed with 4% paraformaldehyde and stained with a monoclonal antibody against pNF-H (1 : 500) (Covance, Emeryville, CA, USA) and polyclonal antibody against c-Fos (1 : 500) (Santa Cruz Biotechnology, Dallas, TX, USA) at  $4^{\circ}\text{C}$  for 20 h. An Alexa Fluor 488-conjugated goat anti-mouse IgG (1 : 300) and Alexa Fluor 568-conjugated goat anti-rabbit antibody (1 : 300) were used as secondary antibodies (Molecular Probes, Eugene, OR, USA). For staining c-Fos, NeuroTrace Fluorescent Nissl Stains (Molecular Probes) was used as counter staining to confirm its neuron-specific expression. The fluorescent images for axons and c-Fos were captured using a fluorescent microscope (BX-61, Olympus, Tokyo, Japan) at  $324 \mu\text{m} \times 430 \mu\text{m}$ . Six successive brain slices from the medial prefrontal cortex and six successive slices from the temporal cortex containing the perirhinal cortex were captured for quantification. The lengths of pNF-H-positive axons were measured using an image analyzer Neurocyte (Kurabo, Osaka, Japan), which automatically traces and measures neurite length without measuring cell bodies. The area of c-Fos-positive staining was measured using the Image J (<http://rsbweb.nih.gov/ij/>).

**In vivo single unit recordings in the mPFC and hippocampal CA1.** C57BL/6 mice (8 weeks old, male) were i.p. administered diosgenin for 21 days and were anesthetized with i.p. injection of urethane (1.5 g/kg; Sigma-Aldrich, Oakville, ON, Canada) and mounted on the stereotaxic apparatus. Body temperature of the animals was maintained with the heat pad during recordings. After incision was given to the skull skin, burr holes were made onto the skull by the dental drill for placements of recording electrodes. Extracellular electrodes were made of 1 mm O.D. Omegadot borosilicate glass tubes (WPI, Sarasota, FL, USA) pulled with the puller. Typical tip resistance of electrodes filled with 2 M NaCl solution was approximately 3 ~ 5 M $\Omega$ . One recording electrode was lowered into the right hemisphere of the layer V–VI of the mPFC (+1.5 mm A/P, +0.4 mm M/L and  $-2.8$  mm D/V). The other recording electrode was aimed at CA1 ( $-2.3$  mm A/P, +1.7 mm M/L and  $-1.5$  mm D/V). Five minutes of single unit recordings were obtained from each animal. Extracellular single unit signals were 10,000 times amplified and band-pass filtered at 0.1–10 kHz with the amplifiers. Analog signals were then digitized with the digitizer and stored in the computer for off-line analysis. Correlation of single unit discharges between the mPFC and CA1 were assessed by coherence analyses, using the functions implemented in the statistical analysis software STATISTICA (StatSoft, Tulsa, OK, USA). All animals were killed rapidly on completion of electrophysiological recordings with an overdose of pentobarbital (100 mg/kg, i.p.), and after cryoprotection of brains in 30% sucrose solution, brains were sectioned at 30  $\mu\text{m}$  thickness with the sliding microtome. Recording and stimulation sites were confirmed with Nissl staining using the light microscope.

**Primary culture.** Embryos were removed from pregnant ddY mice (Japan SLC) at 14 days of gestation. The cortices were dissected, and the dura mater was removed. The tissues were minced, dissociated and cultured with neurobasal medium (Invitrogen, Grand Island, NY, USA) that included B-27 supplement (Invitrogen), 0.6% D-glucose and 2 mM L-glutamine at  $37^{\circ}\text{C}$  in a humidified incubator with 10%  $\text{CO}_2$  on 8-well chamber slides (Falcon, Franklin Lakes, NJ, USA) coated with 5  $\mu\text{g}/\text{ml}$  poly-D-lysine. The seeding cell density was  $2.9 \times 10^4$  cells/cm $^2$ .

**Measurement of axonal density.** Three days after cell seeding, the control antibody (normal rabbit IgG, 1 : 500) or polyclonal anti-rabbit 1,25D $_3$ -MARRS (Ab099 clone, 1 : 500) was applied to the cells. After a 15-min incubation with the antibody, the cells were treated with vehicle solution or diosgenin (1  $\mu\text{M}$ ). The cells were fixed with 4% paraformaldehyde and immunostained at  $4^{\circ}\text{C}$  for 20 h with a monoclonal antibody against pNF-H (1 : 500) as an axonal marker and a polyclonal antibody against MAP2 (1 : 500) as a neuronal marker. Alexa Fluor 488-conjugated goat anti-mouse IgG (1 : 300) and Alexa Fluor 568-conjugated goat anti-rabbit IgG (1 : 300) were used as secondary antibodies. The fluorescent images were captured using a fluorescent microscope system (BX61/DP70, Olympus) at  $324 \mu\text{m} \times 430 \mu\text{m}$ . Twenty-one images were captured per treatment. The lengths of the pNF-H-positive axons were measured using the Neurocyte image analyzer (Kurabo). The sum of the axon lengths was divided by the number of MAP2-positive neurons in an image. The resulting axon density was averaged over all of the images.

**Surgical procedure.** Mice were anesthetized with chloral hydrate (500 mg/kg) and positioned in a stereotaxic apparatus. The scalp was shaved and cut, and the skull was exposed. A cannula (Brain Infusion Kit 3, Alzet, Cupertino, CA, USA) was positioned into a lateral ventricle at the following coordinates:  $-0.22$  mm A/P, +1.0 mm M/L and  $-2.5$  mm D/V. The free end of the cannula was connected to a mini-osmotic pump (Alzet, Model 1007D) via a 3.5-cm piece of polyvinylchloride (PVC) tubing (Alzet). The mini-osmotic pump and connecting PVC tubing were filled with artificial cerebrospinal fluid (aCSF) or anti-1,25D $_3$ -MARRS dissolved in aCSF. The CSF production rate in a mouse is 18  $\mu\text{l}/\text{h}$ . The infusion rate of the mini-osmotic pump was 0.5  $\mu\text{l}/\text{h}$ . Therefore, the anti-1,25D $_3$ -MARRS antibody and aCSF were mixed at 1 : 14 ratio to reach a 1 : 500 dilution, which is the effective dose of the antibody for neutralization. The filled pumps were incubated in sterile saline at  $37^{\circ}\text{C}$  for at least 16 h before being implanted under the dorsal skin of the mouse's back. The cannula base and attached piece of PVC tubing were fixed to the skull with Loctite cyanoacrylic 454. During and after surgery, mice were placed on a heating pad to maintain body temperature.

**Statistical analysis.** Statistical comparisons were performed using one-way analysis of variance (ANOVA) with *post hoc* Dunnett's tests, unpaired *t*-tests and paired *t*-tests in GraphPad Prism 5 (GraphPad Software, La Jolla, CA, USA). Values of  $p < 0.05$  were considered significant. The mean values of the data are presented together with the SE.

- Tohda, C., Urano, T., Umezaki, M., Nemere, I. & Kuboyama, T. Diosgenin is an exogenous activator of 1,25D(3)-MARRS/Pdia3/Erp57 and improves Alzheimer's disease pathologies in 5XFAD mice. *Sci. Rep.* **2**, 535 (2012).
- Yan, L. L., Zhang, Y. J., Gao, W. Y., Man, S. L. & Wang, Y. In vitro and in vivo anticancer activity of steroid saponins of Paris polyphylla var. yunnanensis. *Exp. Oncol.* **31**, 27–32 (2009).
- Huang, C. H., Ku, C. Y. & Jan, T. R. Diosgenin attenuates allergen-induced intestinal inflammation and IgE production in a murine model of food allergy. *Planta Med.* **75**, 1300–1305 (2009).
- Chiu, C. S. *et al.* Diosgenin ameliorates cognition deficit and attenuates oxidative damage in senescent mice induced by D-galactose. *Am. J. Chin. Med.* **39**, 551–563 (2011).
- Kang, T. H. *et al.* Diosgenin from Dioscorea nipponica ameliorates diabetic neuropathy by inducing nerve growth factor. *Biol. Pharm. Bull.* **34**, 1493–1498 (2011).
- Li, F., Fernandez, P. P., Rajendran, P., Hui, K. M. & Sethi, G. Diosgenin, a steroidal saponin, inhibits STAT3 signaling pathway leading to suppression of proliferation and chemosensitization of human hepatocellular carcinoma cells. *Cancer Lett.* **292**, 197–207 (2010).
- Srinivasan, S. *et al.* Diosgenin targets Akt-mediated prosurvival signaling in human breast cancer cells. *Int. J. Cancer* **125**, 961–967 (2009).
- Larsson, B. & Nemere, I. Effect of growth and maturation on membrane-initiated actions of 1,25-dihydroxyvitamin D $_3$ -II: calcium transport, receptor kinetics, and signal transduction in intestine of female chickens. *J. Cell. Biochem.* **90**, 901–913 (2003).
- Rosso, A. *et al.* 1 $\alpha$ ,25(OH) $_2$ -Vitamin D $_3$  stimulates rapid plasma membrane calcium influx via MAPK activation in immature rat Sertoli cells. *Biochimie* **94**, 146–154 (2012).
- Nemere, I., Garbi, N., Hammerling, G. J. & Khanal, R. C. Intestinal cell calcium uptake and the targeted knockout of the 1,25D $_3$ -MARRS (membrane-associated, rapid response steroid-binding) receptor/PDIA3/Erp57. *J. Biol. Chem.* **285**, 31859–31866 (2010).
- Nemere, I. *et al.* Ribozyme knockdown functionally links a 1,25(OH) $_2$ D $_3$  membrane binding protein (1,25D $_3$ -MARRS) and phosphate uptake in intestinal cells. *Proc. Natl. Acad. Sci. U. S. A.* **101**, 7392–7397 (2004).
- Buitrago, C. G., Arango, N. S. & Boland, R. L. 1 $\alpha$ ,25(OH) $_2$ D $_3$ -dependent modulation of Akt in proliferating and differentiating C2C12 skeletal muscle cells. *J. Cell. Biochem.* **113**, 1170–1181 (2012).
- Guo, G. G. *et al.* Association of the chaperone glucose-regulated protein 58 (GRP58/ER-60/Erp57) with Stat3 in cytosol and plasma membrane complexes. *J. Interferon Cytokine Res.* **22**, 555–563 (2002).
- Haussler, M. R., Jurutka, P. W., Mizwicki, M. & Norman, A. W. Vitamin D receptor (VDR)-mediated actions of 1 $\alpha$ ,25(OH) $_2$ vitamin D(3): genomic and non-genomic mechanisms. *Best Pract. Res. Clin. Endocrinol. Metab.* **25**, 543–559 (2011).
- Okamura, W. H. *et al.* Chemistry and conformation of vitamin D molecules. *J. Steroid Biochem. Mol. Biol.* **53**, 603–613 (1995).
- Benedetti, B. L., Takashima, Y., Wen, J. A., Urban-Ciecko, J. & Barth, A. L. Differential wiring of layer 2/3 neurons drives sparse and reliable firing during neocortical development. *Cereb. Cortex* **23**, 2690–2699 (2013).
- Liu, F. *et al.* Activation of estrogen receptor-beta regulates hippocampal synaptic plasticity and improves memory. *Nat. Neurosci.* **11**, 334–343 (2008).
- Kato, T. *et al.* Hepatocyte growth factor overexpression in the nervous system enhances learning and memory performance in mice. *J. Neurosci. Res.* **90**, 1743–1755 (2012).
- Rogers, J. T. *et al.* Reelin supplementation enhances cognitive ability, synaptic plasticity, and dendritic spine density. *Learn. Mem.* **18**, 558–564 (2011).



20. Chen, Q. *et al.* A novel neurotrophic drug for cognitive enhancement and Alzheimer's disease. *PLoS One* **6**, e27865 (2011).
21. Uhlen, M. *et al.* A human protein atlas for normal and cancer tissues based on antibody proteomics. *Mol. Cell. Proteomics* **4**, 1920–1932 (2005).
22. Verma, P. *et al.* Axonal protein synthesis and degradation are necessary for efficient growth cone regeneration. *J. Neurosci.* **25**, 331–342 (2005).
23. Shi, S. H., Jan, L. Y. & Jan, Y. N. Hippocampal neuronal polarity specified by spatially localized mPar3/mPar6 and PI 3-kinase activity. *Cell* **112**, 63–75 (2003).
24. Atwal, J. K., Massie, B., Miller, F. D. & Kaplan, D. R. The TrkB-Shc site signals neuronal survival and local axon growth via MEK and P13-kinase. *Neuron* **27**, 265–277 (2000).
25. Campbell, D. S. & Holt, C. E. Apoptotic pathway and MAPKs differentially regulate chemotropic responses of retinal growth cones. *Neuron* **37**, 939–952 (2003).
26. Aigner, L. *et al.* Overexpression of the neural growth-associated protein GAP-43 induces nerve sprouting in the adult nervous system of transgenic mice. *Cell* **83**, 269–278 (1995).
27. Bouchard, J. F., Horn, K. E., Stroth, T. & Kennedy, T. E. Depolarization recruits DCC to the plasma membrane of embryonic cortical neurons and enhances axon extension in response to netrin-1. *J. Neurochem.* **107**, 398–417 (2008).
28. Brown, J., Bianco, J. I., McGrath, J. J. & Eyles, D. W. 1,25-dihydroxyvitamin D3 induces nerve growth factor, promotes neurite outgrowth and inhibits mitosis in embryonic rat hippocampal neurons. *Neurosci. Lett.* **343**, 139–143 (2003).
29. Briones, T. L. & Darwish, H. Vitamin D mitigates age-related cognitive decline through the modulation of pro-inflammatory state and decrease in amyloid burden. *J. Neuroinflammation* **9**, 244 (2012).
30. Dean, A. J. *et al.* Effects of vitamin D supplementation on cognitive and emotional functioning in young adults—a randomised controlled trial. *PLoS One* **6**, e25966 (2011).
31. Mizwicki, M. T. & Norman, A. W. The vitamin D sterol-vitamin D receptor ensemble model offers unique insights into both genomic and rapid-response signaling. *Science signaling* **2**, re4 (2009).
32. Deeb, K. K., Trump, D. L. & Johnson, C. S. Vitamin D signalling pathways in cancer: potential for anticancer therapeutics. *Nat. Rev. Cancer* **7**, 684–700 (2007).

## Acknowledgments

This work was partially supported by a research grant from the Astellas Foundation for Research on Metabolic Disorders.

## Author contributions

C.T. designed the study, wrote the protocol, wrote the protocol, carried out statistical analyses and experiments except for *in vivo* electrophysiological experiments and prepared the manuscript. Y.L. and Y.G. performed *in vivo* electrophysiological experiments. I.N. prepared and provided the antibody. All authors contributed to and have approved the final manuscript.

## Additional information

**Competing financial interests:** The authors declare no competing financial interests.

**How to cite this article:** Tohda, C., Lee, Y.-A., Goto, Y. & Nemere, I. Diosgenin-induced cognitive enhancement in normal mice is mediated by 1,25D<sub>3</sub>-MARRS. *Sci. Rep.* **3**, 3395; DOI:10.1038/srep03395 (2013).



This work is licensed under a Creative Commons Attribution-NonCommercial-NoDerivs 3.0 Unported license. To view a copy of this license, visit <http://creativecommons.org/licenses/by-nc-nd/3.0>

# SCIENTIFIC REPORTS



## **Corrigendum:** Diosgenin-induced cognitive enhancement in normal mice is mediated by $1,25D_3$ -MARRS

Chihiro Tohda, Young-A. Lee, Yukiiori Goto & Ilka Nemere

*Scientific Reports* 3:3395; doi: 10.1038/srep03395; published online 02 December 2013; updated on 03 August 2015

The Acknowledgements section in this Article is incomplete.

“This work was partially supported by a research grant from the Astellas Foundation for Research on Metabolic Disorders.”

should read:

“This work was partially supported by a research grant from the Astellas Foundation for Research on Metabolic Disorders(C.T.), and by a Grant-in-Aid for the Cooperative Research Project from Joint Usage/Research Center(Joint Usage/Research Center for Science-Based Natural Medicine) Institute of Natural Medicine, University of Toyama in 2011 (C.T., Y.G. and Y-A.L.)”